First publ. in: Optics Express 19 (2011), 2, pp. 1641-1647
doi:10.1364/OE.19.001641

Ultraviolet photoluminescence of ZnO quantum dots sputtered at room-temperature

Gillian Kiliani,[1] Reinhard Schneider,[2] Dimitri Litvinov,[2] Dagmar Gerthsen,[2] Mikhail Fonin,[1] Ulrich Rüdiger,[1] Alfred Leitenstorfer,[1] and Rudolf Bratschitsch[1,*]

[1] *Department of Physics and Center for Applied Photonics, University of Konstanz, D-78464 Konstanz, Germany*
[2] *Laboratorium für Elektronenmikroskopie, Karlsruher Institut für Technologie, D-76131 Karlsruhe, Germany*

[*] *rudolf.bratschitsch@uni-konstanz.de*

Abstract: We observe ultraviolet photoluminescence from sputtered ZnO quantum dots which are fabricated with no annealing steps. The nanocrystals are embedded in amorphous SiO_2 and exhibit a narrow size distribution of 3.5 ± 0.6 nm. Photoluminescence and transmittance measurements show a shift of ultraviolet emission and absorption of the dots compared to bulk ZnO material. This work paves the way for cheap nanooptical devices in the ultraviolet which are fabricated in a single sputtering run.

© 2011 Optical Society of America

OCIS codes: (220.4241) Nanostructure fabrication; (260.7190) Ultraviolet.

References and links

1. N. Janßen, K. M. Whitaker, D. R. Gamelin, and R. Bratschitsch, "Ultrafast spin dynamics in colloidal ZnO quantum dots," Nano Lett. **8**, 1991–1994 (2008).
2. S. Kako, C. Santori, K. Hoshino, S. Götzinger, Y. Yamamoto, and Y. Arakawa, "A gallium nitride single-photon source operating at 200 K," Nature Mater **5**, 887–892 (2006).
3. T. Thomay, T. Hanke, M. Tomas, F. Sotier, K. Beha, V. Knittel, M. Kahl, K. M. Whitaker, D. R. Gamelin, A. Leitenstorfer, and R. Bratschitsch, "Colloidal ZnO quantum dots in ultraviolet pillar microcavities," Opt. Express **16**, 9791–9794 (2008).
4. J. G. Ma, Y. C. Liu, C. S. Xu, Y. X. Liu, C. L. Shao, H. Y. Xu, J. Y. Zhang, Y. M. Lu, D. Z. Shen, and X. W. Fan, "Preparation and characterization of ZnO particles embedded in SiO_2 matrix by reactive magnetron sputtering," J. Appl. Phys. **97**, 103509 (2005).
5. G. Mayer, M. Fonin, U. Rüdiger, R. Schneider, D. Gerthsen, N. Janßen, and R. Bratschitsch, "The structure and optical properties of ZnO nanocrystals embedded in SiO_2 fabricated by radio-frequency sputtering," Nanotechnology **20**, 075601 (2009).
6. V. Pankratov, V. Osinniy, A. Nylandsted Larsen, and B. Bech Nielsen, "ZnO nanocrystals/SiO_2 multilayer structures fabricated by rf-magnetron sputtering," Physica B **404**, 4827–4830 (2009).
7. J. I. Pankove, *Optical Processes in Semiconductors* (Prentice-Hall Inc., 1971).
8. S. Srinivasan, F. Bertram, A. Bell, F. A. Ponce, S. Tanaka, H. Omiya, and Y. Nakagawa, "Low Stokes shift in thick and homogeneous InGaN epilayers," Appl. Phys. Lett. **80**, 550–552 (2002).
9. P.-T. Hsieh, Y.-C. Chen, C.-M. Wang, Y.-Z. Tsai, and C.-C. Hu, "Structural and photoluminescence characteristics of ZnO films by room temperature sputtering and rapid thermal annealing process," Appl. Phys. A **84**, 345–349 (2006).
10. Y. G. Wang, S. P. Lau, H. W. Lee, S. F. Yu, B. K. Tay, X. H. Zhang, and H. H. Hng, "Photoluminescence study of ZnO films prepared by thermal oxidation of Zn metallic films in air," J. Appl. Phys. **94**, 354–358 (2003).
11. J. Zhao, L. Hu, Z. Wang, Y. Zhao, X. Liang, and M. Wang, "High-quality ZnO thin films prepared by low temperature oxidation of metallic Zn," Appl. Surf. Sci. **229**, 311–315 (2004).

#138828 - $15.00 USD Received 8 Dec 2010; revised 3 Jan 2011; accepted 3 Jan 2011; published 13 Jan 2011
(C) 2011 OSA

Konstanzer Online-Publikations-System (KOPS)
URN: http://nbn-resolving.de/urn:nbn:de:bsz:352-opus-129421
URL: http://kops.ub.uni-konstanz.de/volltexte/2011/12942

12. Y. Chen, D. M. Bagnall, H.-J. Koh, K.-T. Park, K. Hiraga, Z. Zhu, and T. Yao, "Plasma assisted molecular beam epitaxy of ZnO on *c*-plane sapphire: growth and characterization," J. Appl. Phys. **84**, 3912–3918 (1998).
13. V. A. Fonoberov, K. A. Alim, and A. A. Balandin, "Photoluminescence investigation of the carrier recombination processes in ZnO quantum dots and nanocrystals," Phys. Rev. B **73**, 165317 (2006).
14. K. Vanheusden, W. L. Warren, C. H. Seager, D. R. Tallant, J. A. Voigt, and B. E. Gnade, "Mechanisms behind green photoluminescence in ZnO phosphor powders," J. Appl. Phys. **79**, 7983–7990 (1996).
15. M. K. Wu, Y. T. Shih, M. J. Chen, J. R. Yang, and M. Shiojiri, "ZnO quantum dots embedded in a SiO_2 nanoparticle layer grown by atomic layer deposition," Phys. Status Solidi (RRL) **3**, 88–90 (2009).
16. J. G. Lu, Z. Z. Ye, Y. Z. Zhang, Q. L. Liang, S. Fujita, and Z. L. Wang, "Self-assembled ZnO quantum dots with tunable optical properties," Appl. Phys. Lett. **89**, 023122 (2006).
17. L. Mädler, J. W. Stark, and S. E. Pratsinis, "Rapid synthesis of stable ZnO quantum dots," J. Appl. Phys. **92**, 6537–6540 (2002).
18. K. Suzuki, H. Kondo, M. Inoguchi, N. Tanaka, K. Kageyama, and H. Takagi, "Optical properties of well-crystallized and size-tuned ZnO quantum dots," Appl. Phys. Lett. **94**, 223103 (2009).
19. R. T. Senger and K. K. Bajaj, "Optical properties of confined polaronic excitons in spherical ionic quantum dots," Phys. Rev. B **68**, 045313 (2003).
20. L. E. Brus, "Electron-electron and electron-hole interactions in small semiconductor crystallites: the size dependence of the lowest excited electronic state," J. Chem. Phys. **80**, 4403–4409 (1984).
21. M. Iwamatsu, M. Fujiwara, N. Happo, and K. Horii, "Effects of dielectric discontinuity on the ground-state energy of charged Si dots covered with a SiO_2 layer," J. Phys.: Condens. Matter **9**, 9881–9892 (1997).
22. V. A. Fonoberov and A. A. Balandin, "Origin of ultraviolet photoluminescence in ZnO quantum dots: confined excitons versus surface-bound impurity exciton complexes," Appl. Phys. Lett. **85**, 5971–5973 (2004).
23. V. A. Fonoberov and A. A. Balandin, "Radiative lifetime of excitons in ZnO nanocrystals: the dead-layer effect," Phys. Rev. B **70**, 195410 (2004).
24. K. A. Alim, V. A. Fonoberov, and A. A. Balandin, "Origin of the optical phonon frequency shifts in ZnO quantum dots," Appl. Phys. Lett. **86**, 053103 (2005).
25. Y. Yamada, *Wide Bandgap Semiconductors*, 1st ed. (Springer, Berlin, 2007).

Zinc oxide (ZnO) is a direct semiconductor with a wide bandgap of 3.4 eV. Therefore, it is a promising candidate for ultraviolet (UV) single-photon and opto-spintronic applications [1]. An important objective in this area is the fabrication of an efficient single-photon source in the UV for free-space quantum communications and calibration purposes [2]. To increase its efficiency, a monolithic system consisting of a UV nanoemitter located inside an optical cavity is beneficial. Recently, colloidal ZnO quantum dots have been successfully embedded in a dielectric pillar microcavity by combining radio-frequency sputtering and wet chemical preparation steps [3]. However, a monolithic device consisting of both sputtered dielectric Bragg mirrors and sputtered ZnO quantum dots fabricated in one single process would be highly desirable – similar to the simple production of computer hard drives via sputtering. Today, ZnO quantum dots embedded in SiO_2 surroundings [4, 5, 6] as well as planar UV microcavities made of dielectric Bragg mirrors [3] may be readily fabricated via magnetron sputtering. However, thermal annealing is necessary up till now to prepare ZnO quantum dots showing UV emission. Such steps would lead to the degradation of the device. For example, thermally induced interdiffusion among the alternating dielectric layers degrades the Bragg mirrors and hence the performance of the optical cavity. This work demonstrates that ZnO quantum dots showing the desired photon emission in the UV can be prepared by sputtering without annealing.

ZnO quantum dots are fabricated by reactive radio frequency magnetron sputtering of ZnO and SiO_2 multilayers onto Al_2O_3(0001) and Si(001) substrates or carbon-coated Cu grids. A high vacuum base pressure of 2.5×10^{-8} Torr ensures a stable and clean deposition environment. Si and ZnO targets are used at sputtering powers of 200 W and 30 W, respectively. The sputtering process is carried out in Ar (15 sccm) and O_2 (3 sccm) atmosphere. The working pressure is kept at 1.5 mTorr for deposition of SiO_2 and at 5 mTorr for deposition of ZnO. The entire fabrication process is carried out at room-temperature with no annealing steps.

Fig. 1(a) illustrates the sample structure. First, a SiO_2 bottom layer of 15 nm thickness is deposited onto the Al_2O_3(0001) or Si(001) substrates to eliminate any influence of the substrate

#138828 - $15.00 USD Received 8 Dec 2010; revised 3 Jan 2011; accepted 3 Jan 2011; published 13 Jan 2011
(C) 2011 OSA

on the growth of the quantum dots. The bottom layer is followed by ten alternating layers of ZnO (2 nm nominal thickness) and SiO_2 (5 nm nominal thickness) resulting in a total film thickness of 85 nm. Microstructural investigations of the sputter-deposited ZnO quantum dots are performed by high resolution transmission electron microscopy (HRTEM) using a Philips CM 200 FEG ST microscope at 200 kV acceleration voltage. Fig. 1(b) shows a representative HRTEM image (side-view) of the nominally 2-nm-thick ZnO layers embedded in amorphous SiO_2. ZnO quantum dots may be identified as dark regions within the bright SiO_2 surroundings.

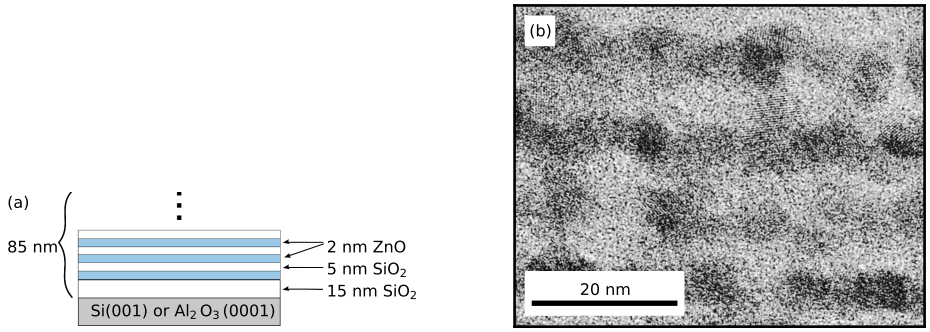

Fig. 1. (Color online) (a) Schematic drawing of the sputtered SiO_2/ZnO multilayer structure. (b) Corresponding HRTEM side-view image of ZnO quantum dots embedded in SiO_2 deposited onto Si(001).

Compared to the amorphous SiO_2, the dark ZnO regions show a stripe-like structure proving the crystallinity of the material. ZnO regions do not appear as connected layers, but as separated quantum dots. Their diameters, however, are difficult to estimate from these HRTEM side-view images since the quantum dots are arranged behind each other.

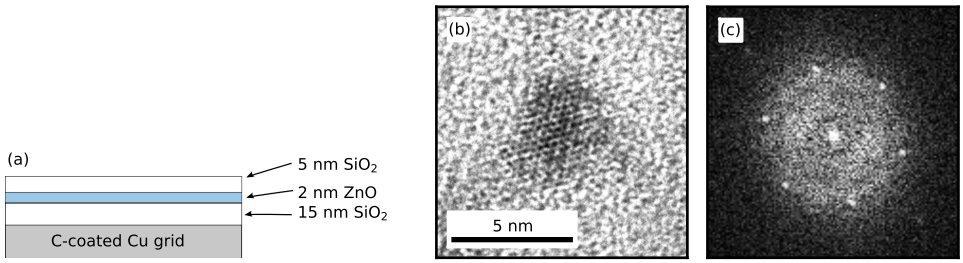

Fig. 2. (Color online) (a) Schematic drawing of the sputtered SiO_2(10 nm)/ZnO(2 nm)/SiO_2(5 nm) trilayer structure deposited onto a carbon-coated Cu grid. (b) HRTEM top-view image of a single ZnO quantum dot embedded in amorphous SiO_2. (c) Diffractogram corresponding to (b).

Therefore, additional microstructural investigations by HRTEM are performed on a single SiO_2(10 nm)/ZnO(2 nm)/SiO_2(5 nm) trilayer which is deposited onto a carbon-coated Cu grid (Fig. 2(a)) with the same preparation conditions. This sample allows for top-view HRTEM images of single ZnO quantum dots and an evaluation of their size distribution. Fig. 2(a) presents a schematic drawing of the sample structure. Fig. 2(b) shows a HRTEM image of a single ZnO quantum dot with a diameter of 4 nm embedded in SiO_2. While the SiO_2 surroundings

#138828 - $15.00 USD Received 8 Dec 2010; revised 3 Jan 2011; accepted 3 Jan 2011; published 13 Jan 2011
(C) 2011 OSA

are amorphous, the ZnO quantum dot shows a hexagonal crystal structure. The crystallinity is confirmed by the diffractogram (Fig. 2(c)), which corresponds to the HRTEM image.

Fig. 3(a) shows a representative top-view HRTEM image of ZnO quantum dots embedded in SiO_2. In this image the quantum dots are well separated. Evaluation of several HRTEM images allows counting the ZnO quantum dots with a resolution of 1 nm in diameter. This leads to the size distribution presented in Fig. 3(b). The average quantum dot diameter is 3.5 ± 0.6 nm, i. e. the sputtered quantum dots are almost monodisperse. No quantum dots with a diameter less than 2 nm or larger than 5 nm are found. This size distribution is comparable or even narrower than that of sputtered, but annealed, ZnO quantum dots [5, 6]. Our measurements on the trilayer also prove that the formation of the ZnO quantum dots does not depend on the number of sputtered layers. This fact is important, since for optimum light-matter coupling only a single layer of quantum dots should be placed in the antinode of an optical microcavity.

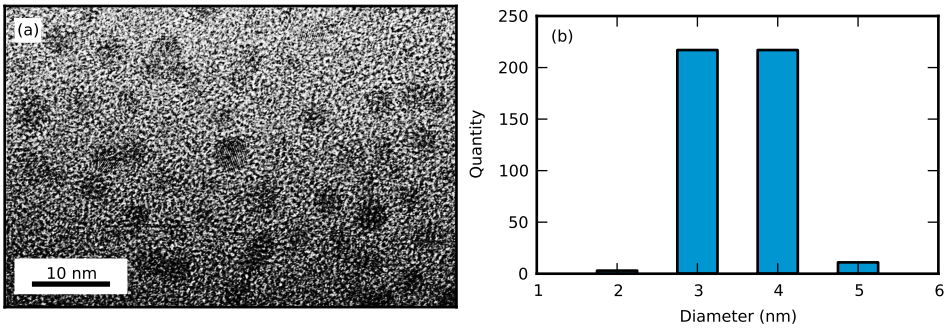

Fig. 3. (Color online) (a) Top-view HRTEM image of a single layer of ZnO quantum dots embedded in amorphous SiO_2. (b) histogramm of the size distribution of the sputtered ZnO quantum dots.

To investigate the optical properties of the sputtered ZnO quantum dots, measurements of the optical transmittance in the visible and UV are performed on the multilayered sample deposited on a transparent sapphire substrate. For this measurement we use an Agilent 8453E UV-visible spectrometer with a spectral resolution of 1 nm. Fig. 4 shows the square of the optical absorption coefficient α of the ZnO quantum dots at room-temperature extracted from the transmittance T by $\alpha = -\ln(T)/d$, where $d = 10 \times 2$ nm $= 20$ nm denotes the effective ZnO layer thickness. It can be seen that absorption sets in above 3.5 eV.

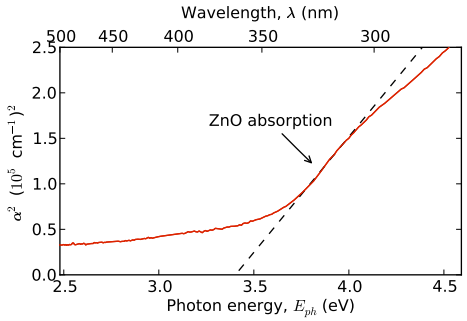

Fig. 4. (Color online) Square of the optical absorption coefficient vs. photon energy of the ZnO quantum dots, demonstrating the onset of absorption above 3.5 eV.

#138828 - $15.00 USD Received 8 Dec 2010; revised 3 Jan 2011; accepted 3 Jan 2011; published 13 Jan 2011
(C) 2011 OSA

Assuming direct transitions for a semiconductor with parabolic bands, the bandgap E_g may be extracted from $\alpha = A \cdot \sqrt{h\nu - E_g}$, where A is a constant and $h\nu$ is the photon energy [7]. Thus, the bandgap may be obtained by extrapolation of the linear part of α^2 to the energy axis, leading to $E_g^{\mathrm{QD}} = 3.40(2)$ eV. Note that this simplified model does not account for excitonic effects and therefore slightly underestimates the bandgap [8].

To directly compare the optical properties of the ZnO quantum dots with bulk ZnO, a reference sample consisting of a thick ZnO layer (330 nm) has been prepared by sputtering. It is deposited at room-temperature, but annealed for 3 h at 500 °C in 5 sccm O_2 and 20 sccm N_2. Similiar thin-film preparation procedures, involving annealing steps between 400 °C and 600 °C, have been reported earlier to result in strong UV emission between 3.27 eV and 3.31 eV and suppression of defect photoluminescence in bulk ZnO [9, 10, 11]. Evaluation of the optical transmittance (not shown) of the 330 nm ZnO layer results in a bandgap of $E_g^{\mathrm{bulk}} = 3.28(1)$ eV. When comparing the two retrieved bandgap values for bulk ZnO and ZnO quantum dots, we find a large blueshift of 120 meV which will be addressed later.

To demonstrate the ability of the sputtered quantum dots to serve as light emitters in the UV, we perform photoluminescence emission measurements. The sample is optically excited by a HeCd laser (P_{ex} = 0.5 mW) at a wavelength of 325 nm. The room-temperature photoluminescence spectrum of the ZnO quantum dots in Fig. 5(a) clearly displays UV emission centered at $E_{\mathrm{PL}}^{\mathrm{QD}} = 3.31$ eV with a full width at half maximum (FWHM) of 83 meV. This UV emission is usually attributed to free exciton transitions [4, 12]. The FWHM is comparable to that of high-quality bulk ZnO which shows a typical FWHM of 80 meV to 120 meV and is evidence for the good crystalline quality of the sample [10, 11, 12, 13]. The additional broad emission band in the visible region of the spectrum is attributed to electron-hole recombination of oxygen vacancies [14]. To our knowledge this is the first report of UV emission at room-temperature from non-annealed sputtered ZnO quantum dots. In our fabrication process, the high crystalline quality and few surface defects needed to exhibit UV emission at room-temperature are achieved by using low sputtering rates of about 0.05 Å/s.

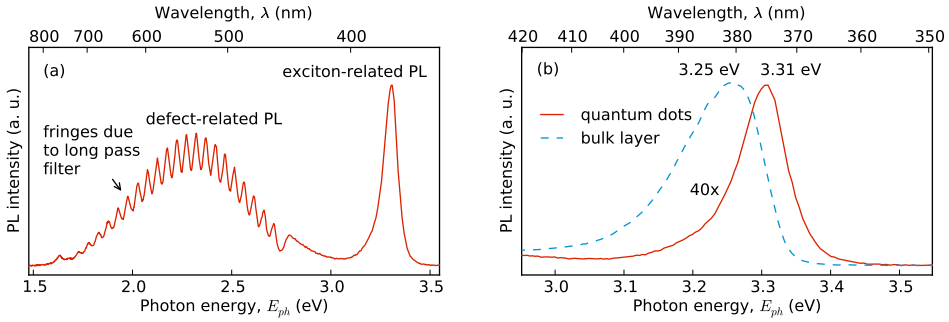

Fig. 5. (Color online) (a) Room-temperature photoluminescence (PL) spectrum of the ZnO quantum dots showing UV exciton-related as well as visible defect-related emission. (b) Comparison of UV photoluminescence emission of the sputtered ZnO quantum dots with a sputtered and annealed bulk ZnO layer of 330 nm thickness.

Fig. 5(b) depicts the UV emission of the ZnO quantum dots compared to the UV emission of the sputtered bulk ZnO layer. Similiar to the transmittance measurements, the photoluminescence emission of the quantum dots at 3.31 eV shows a prominent blueshift compared to photoluminescence emission of 3.25 eV of the ZnO bulk layer. However, with 60 meV the shift is less pronounced than in transmittance measurements. We attribute the observed blueshift observed both in transmittance and photoluminescence measurements of ZnO quantum dots

#138828 - $15.00 USD Received 8 Dec 2010; revised 3 Jan 2011; accepted 3 Jan 2011; published 13 Jan 2011
(C) 2011 OSA

compared to bulk material to quantum confinement [4, 15, 16, 17, 18]. Since the exciton Bohr radius in ZnO is 2.34 nm [19], our quantum dots with a diameter of 3.5 ± 0.6 nm are in the moderate confinement regime. Assuming free-standing spherical ZnO quantum dots, the shift of interband transitions due to confinement for a dot diameter of 3.5 nm may be estimated using the model of Brus [20] to be 300 meV. Electron and hole effective masses and the permittivity of ZnO are taken from [19]. The calculated value is larger than our observed one of 120 meV. This discrepancy might be explained by the strong change of energy shift within only a small range of quantum dot diameter: the theoretical shift due to quantum confinement for ZnO quantum dots with a diameter of 2 nm is 1.40 eV, while it is only 70 meV for 5 nm ZnO quantum dots. Additional contributions to the blueshift could be caused by the confinement due to charges inside the quantum dots or dielectric surroundings [21].

Fonoberov *et al.* theoretically investigated the UV photoluminescence emission in ZnO nanocrystals with diameters between $2-6$ nm, originating either from confined excitons or possible surface-bound ionized acceptor-exciton complexes [22]. The computed energy shifts cannot be directly compared to our experimental data, since the calculations have been performed for ZnO quantum dots with either water or air as ambient media, but not with SiO_2 surroundings. However, radiative lifetime measurements of the exciton might unambiguously distinguish between quantum confinement or surface-bound exciton states [13, 22, 23, 24].

We not only find energy shifts of the onset of transmission and UV photoluminescence emission of the ZnO quantum dots with respect to bulk material. We also observe a Stokes shift, i. e. an energy difference between absorption and emission $(= E_g^{\mathrm{QD}} - E_{\mathrm{PL}}^{\mathrm{QD}})$ of the ZnO quantum dots, which amounts to 90 meV (Fig. 6). This value agrees well with Stokes shifts of slightly larger ZnO quantum dots observed ealier [16]. The Stokes shift is caused by the inhomogenous broadening of the exciton density of states [25] due to the slightly different sizes of the ZnO quantum dots. In photoluminescence measurements, excitons are generated after relaxation processes at the low-energy side of the inhomogeneously broadened quantum dot ensemble. In contrast, absorption appears over the entire energy range leading to the observed energy shift between absorption and emission: while strong absorption sets in above 3.5 eV, the excitonic photoluminescence emission can be observed at lower energies where the absorption is still weak.

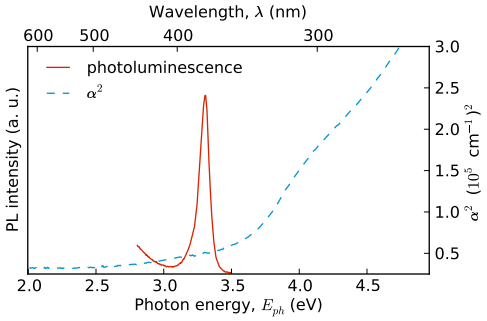

Fig. 6. (Color online) Square of the optical absorption coefficient and UV photoluminescence of ZnO quantum dots, illustrating the Stokes shift.

In summary, ZnO quantum dots with an average diameter of 3.5 ± 0.6 nm showing room-temperature UV photoluminescence were prepared for the first time by magnetron sputtering without any annealing steps. This important improvement allows for the fabrication of nanooptical devices such as microcavities with incorporated ZnO quantum dots in a single sputtering run. The crystallinity and narrow size distribution of the prepared quantum dots are verified by

#138828 - $15.00 USD Received 8 Dec 2010; revised 3 Jan 2011; accepted 3 Jan 2011; published 13 Jan 2011
(C) 2011 OSA

HRTEM imaging. Room-temperature photoluminescence spectra show the characteristic free exciton UV emission which has not been observed for room-temperature-sputtered ZnO quantum dots before. Optical transmittance and photoluminescence spectra both show a blueshift of the quantum dot absorption and emission, respectivly, as compared to bulk ZnO material. This finding is attributed to moderate quantum confinement.

Acknowledgements

We gratefully acknowledge financial support of the Deutsche Forschungsgemeinschaft (DFG) via priority program SPP 1285. G. K. acknowledges financial support of the Carl Zeiss Stiftung. R. B. acknowledges support of the Zukunftskolleg of the University of Konstanz.

#138828 - $15.00 USD Received 8 Dec 2010; revised 3 Jan 2011; accepted 3 Jan 2011; published 13 Jan 2011
(C) 2011 OSA